



# OPEN Experimental study of cerebral edema and expression of VEGF and AQP4 in the penumbra area of rat brain trauma

Li Ai<sup>1,3</sup>, Muhammad Usman<sup>1,2,3</sup> & Hong Lu<sup>1</sup>✉

Traumatic brain injury (TBI) has a high disability rate and a high fatality rate. Traumatic penumbra (TP) is a potentially reversible area around the core area of brain trauma with cerebral edema as the main pathological change, which is a breakthrough to improve the prognosis of patients with TBI and reduce the mortality and disability rate of TBI. Unfortunately, the pathophysiological mechanism of TP is still not fully understood. In this study, we established a moderate traumatic brain injury model in rats and detected pathological molecular markers in TP. Protein content of IgG, VEGF, and AQP4 were detected respectively by HE, Immunofluorescence, and western blot. To investigate the time-varying characteristics of TP, to provide a reference for research and development and screening of TBI targeted drugs. Our experiment showed mainly intracellular edema and vascular edema in TP, first intracellular then vascular edema was dominant. IgG, VEGF, and AQP4 in TP increased significantly. On the second day, AQP4 decreased, and third day AQP4 increased again. We found that in the early stage of TBI cerebral edema developed and it is related to the increase of BBB permeability, upregulation of VEGF and AQP4. Suggesting potential targets for treatment of TP.

**Keywords** Traumatic penumbra, Cerebral edema, BBB, VEGF, AQP4

Traumatic brain injury (TBI) involves a chain reaction initiated by an impact to the head that spreads throughout the brain, often resulting in neurological impairment<sup>1</sup>. It can result in short-term or long-term consequences of varying severity<sup>2,3</sup>. Approximately 70 million individuals worldwide experience traumatic brain injury (TBI) each year<sup>4</sup>, primarily affecting children, young men, and the elderly<sup>5,6</sup>. This places enormous pressure on the global economy, causes physical and psychological harm to patients and their families, and poses significant challenges to public health. The traumatic penumbra (TP) is a secondary, reversible injury zone located between the traumatic core and normal brain tissue following brain trauma. It is primarily characterized by cerebral edema as its main pathological feature. Imaging typically reveals a region of low perfusion, demonstrated by mismatched diffusion-weighted imaging (DWI) and susceptibility-weighted imaging (SWI) sequences<sup>7</sup>. Hematoxylin and eosin (HE) staining shows a variably wide, lightly stained band surrounding the traumatic core area<sup>7</sup>. Therefore, the traumatic penumbra (TP) represents a critical area for targeted treatment of traumatic brain injury (TBI) and is a major focus of medical attention and research. Recent studies on TP have yielded valuable insights, highlighting cerebral edema as its primary pathological feature. This edema includes both vascular and intracellular types, with vascular cerebral edema occurring first, followed by intracellular edema<sup>7</sup>. However, the molecular mechanisms underlying the formation and progression of cerebral edema in the traumatic penumbra (TP) remain incompletely understood, and effective targeted therapies are currently lacking. This study aims to examine pathological changes in the TP of rats following moderate brain trauma by evaluating blood-brain barrier permeability and measuring the expression levels of VEGF and AQP4. By clarifying the time-dependent characteristics of TP, the study intends to elucidate potential molecular mechanisms involved in edema formation and development, identify therapeutic targets for traumatic brain injury (TBI), and ultimately provide insights that support the discovery and development of targeted TBI treatments.

<sup>1</sup>Department of Postdoctoral Research Workstation, Central Hospital Affiliated to Chongqing University of Technology, Chongqing University of Technology, Gonglian yicun No.1 street Iijiatuo, Banan district, Chongqing 400054, P.R. China. <sup>2</sup>Department of Postdoctoral Research Workstation, Kunming Children's Hospital, 28 Shulin St, Kunming, Yunnan, China. <sup>3</sup>Li Ai and Muhammad Usman contributed equally to this work. ✉email: 471739847@qq.com

## Materials and methods

### Animals and groups

A total of 72 healthy male Wistar rats (Spafu (Beijing) Biotechnology Co., Ltd., animal production license number: SCXK (Jing) 2019-0010), aged 7–8 weeks and weighing between 200 and 220 g, were selected for this study. These rats were randomly divided into three groups: control group ( $n=24$ ), sham group ( $n=24$ ), and traumatic brain injury (TBI) group ( $n=24$ ). Each group was further subdivided into three time-point groups: TBI 1-day group ( $n=8$ ), TBI 2-day group ( $n=8$ ), and TBI 3-day group ( $n=8$ ).

All laboratory animals were handled according to the relevant provisions of GB/T35892-2018 and the “Guidelines for the Management and Use of Laboratory Animals” (8th Edition). Ethical approval was obtained from the Ethics and Welfare Committee for Laboratory Animals at Chongqing University of Technology (Approval No. 2024-045). The study was reported following the ARRIVE guidelines.

### Establishing rat model of moderate brain trauma

A model of moderate brain trauma in rats was established using a modified Feeney method<sup>8</sup>. Rats were anesthetized intraperitoneally with 2.5% tribromoethanol at a dose of 10 mL/kg. Each rat was then placed on the experimental operating table in a prone position, and the head was shaved and disinfected. A 2-cm vertical incision was made along the midline between the ears. Subcutaneous soft tissues were carefully separated layer by layer until the skull was exposed. A rechargeable electric drill with a 3.2-mm diameter bit, set to a speed of 1500 rpm, was used to create a bone window. The bone window, measuring 4 mm in diameter, was drilled 2.5 mm posterior to the bregma and 2.5 mm to the left of the midline, and the bone fragments were carefully removed. Next, the rat was positioned and securely fixed in a stereotactic device in a prone orientation. The impaction head of the pneumatic cortical impactor (PSI) was precisely aligned with the exposed bone window. The moderate brain trauma was induced with the following parameters: an impact velocity of 2.5 m/s, an impact dwell time of 0.1 s, an impact depth of 4 mm into the brain tissue, and an impact head diameter of 4 mm. Following the injury, the bone window was closed, and standard debridement and suturing were performed. In the sham group, all procedures were identical to those in the traumatic brain injury (TBI) group, except that craniocerebral impaction was omitted. No interventions were performed in the control group.

### Preparation of paraffin sections

Three rats from each subgroup were selected for paraffin section preparation. Rats were euthanized, by administering an overdose of 2.5% tribromoethanol resulting in unconsciousness and then given cardiac perfusion which lead to subsequent death. The anesthetized rats were fixed in a supine position on the dissection bench. The abdomen was disinfected, and an incision was made to expose the liver. Next, the chest cavity was opened to reveal the heart and lung tissues.

The pericardium was carefully separated, and a perfusion needle was inserted into the left ventricle. An incision was made in the right atrial appendage to allow drainage, and normal saline was perfused through the left ventricle. Once the fluid flowing from the incision changed from red to clear and the liver's color transitioned from dark red to pink, 4% paraformaldehyde was perfused until the tail and limbs became stiff.

Subsequently, the head was removed, and the brain was extracted. The fresh brain tissue was immersed in 4% paraformaldehyde for external fixation for 24 h. Following fixation, the brain tissue was sectioned coronally at the maximum diameter of the trauma center. The brain sections were conventionally embedded in paraffin and sliced into 5  $\mu$ m-thick sections using a paraffin microtome.

### Hematoxylin-eosin (HE)-staining

The Selected paraffin sections were placed in an incubator at 60 °C and dried for 2 h. Subsequently, the sections underwent dewaxing using xylene, followed by rehydration through a graded series of alcohol solutions from high to low concentration until they reached water. Next, the sections were stained with hematoxylin for 3 to 5 min, rinsed with tap water for 5 min to develop the blue coloration, differentiated using 1% hydrochloric acid alcohol for 1 to 3 s, and again rinsed in tap water for another 5 min to restore the blue coloration. Afterward, sections were stained with eosin for 2 min to visualize the cytoplasm. The stained sections were dehydrated through an ascending series of alcohol solutions (from low to high concentration), cleared with xylene, dried, and finally sealed. The target regions (TP regions) were then observed and photographed under an optical microscope.

### AQP4 and glial fibrillary acidic protein (GFAP) Immunofluorescence staining

Paraffin sections were baked, dried, dewaxed, hydrated, and then washed three times with PBS buffer for 3 min each. Antigen retrieval was performed using a microwave, followed by another PBS buffer rinse. Next, sections were treated dropwise with Triton (1:100 dilution) and incubated at room temperature in the dark for 20 min. Sections were rinsed again with PBS buffer, after which endogenous peroxidase blocker was applied dropwise and incubated in the dark at room temperature for another 20 min, followed by a PBS rinse.

Normal goat serum working solution was then applied for blocking at room temperature for 30 min. After removal of the blocking solution, 50  $\mu$ L of primary monoclonal antibodies (rabbit anti-AQP4-IgG at 1:300 dilution and mouse anti-GFAP-IgG at 1:300 dilution) were added and incubated overnight at 4 °C.

On the following day, sections were warmed at 37 °C for 1.5 h and rinsed with PBS buffer. Subsequently, 40–50  $\mu$ L of secondary antibody solution [sheep anti-rabbit IgG-cy3 (1:200 dilution) and sheep anti-mouse IgG-488 (1:100 dilution)] was added and incubated at 37 °C for 1 h. Afterward, sections were rinsed with PBS buffer, stained with DAPI (4', 6-diamidino-2-phenylindole) drops, incubated at 37 °C for 15 min, rinsed again with PBS, and air-dried. Finally, anti-bleaching mounting medium was applied, and the sections were sealed with coverslips. Images were captured using an inverted fluorescence microscope.

### Western blot detected the protein contents of IgG, VEGF and AQP4 in TP

Fresh brain tissues were collected and placed into 1.5 mL EP tubes containing lysis buffer (10 mL buffer with one tablet of protease/phosphatase inhibitor added). The tissues were then homogenized and centrifuged at 12,000 rpm for 15 min at 4 °C, and the supernatant was collected. Total proteins were extracted using radioimmunoprecipitation assay (RIPA) buffer, and their concentrations were measured with the Coomassie Brilliant Blue method to determine the appropriate loading amounts.

Protein samples were boiled at 100 °C for 5 min, cooled, centrifuged at 10,000 rpm, and stored. Samples (10 µL/lane, 50 µg/well) underwent gel electrophoresis at 120 V for 30 min, followed by 60 V for 4 h. Subsequently, proteins were transferred onto PVDF membranes at a constant current of 0.3 A for 55 min. The membranes were blocked in 5.0% bovine serum albumin (BSA) for 2 h at room temperature and then incubated overnight at 4 °C.

The following day, membranes were washed twice for 15 min each. Primary antibodies (rabbit anti-IgG, 1:1000, #ab133470, Abcam; rabbit anti-mouse VEGF-A-IgG, 1:1000, #ab214424, Abcam; rabbit anti-mouse AQP4-IgG, 1:1000, #ab128906, Abcam) were prepared in 3% BSA according to manufacturer's instructions. Membranes were incubated in the primary antibody solution for 1 h at room temperature with gentle shaking at 100 rpm. Afterward, membranes were washed four times with PBS (0.01 M, pH 7.2), incubated with secondary antibodies for 45 min, and then washed another four times. Detection was performed using a chemiluminescent substrate kit in a dark room. ImageJ software was used to analyze the target protein bands, with relative protein expression quantified based on grayscale values.

### Statistical analysis

Statistical analyses were performed using SPSS 26.0 software (IBM Corp., USA), and data visualization was conducted using GraphPad Prism 8.0 (GraphPad Software, USA). All measured data are presented as mean  $\pm$  standard deviation (SD). For comparisons involving multiple samples, data that did not follow a normal distribution were analyzed using a non-parametric test for K independent samples. For normally distributed data with homogeneity of variance, one-way ANOVA followed by LSD post-hoc analysis was applied, with  $p$ -values  $< 0.05$  considered statistically significant. If data followed a normal distribution but did not meet variance homogeneity assumptions, the Brown-Forsythe or Welch tests were used.

## Results

### Pathological manifestations of brain tissue in TP

The morphology and structure of brain tissue cells appeared normal in both the control and Sham groups. In the TBI group, mixed edema consisting of vascular edema and intracellular edema was observed in the TP region at various time points. These two types of edema exhibited dynamic changes over time. Intracellular edema predominated at 1 day and 3 days post-TBI, whereas vascular cerebral edema was more prominent at 2 days post-TBI (Fig. 1).

### Protein content of IgG in TP

In the TBI group, IgG protein content in the TP region increased rapidly at 1 day post-injury ( $7.06 \pm 1.80$ ), continued to rise at 2 days ( $9.90 \pm 1.94$ ), and then decreased at 3 days ( $8.01 \pm 1.60$ ). Compared to the control and Sham groups, the IgG expression levels in the TBI group were significantly higher at all measured time points ( $###p < 0.001$ ). Within the TBI group, a significant difference was observed between the 1-day and 2-day post-injury groups ( $*p < 0.05$ ). However, there was no significant difference between the 3-day group and either the 1-day or 2-day groups ( $p > 0.05$ ) (Fig. 2).

### Protein content of VEGF in TP

In the TBI group, VEGF expression levels in the TP region increased at 1 day post-injury ( $2.78 \pm 0.31$ ), peaked at 2 days ( $7.06 \pm 1.04$ ), and subsequently decreased at 3 days ( $3.07 \pm 0.70$ ), returning close to the levels observed at 1 day. Compared to the control and Sham groups, VEGF expression was significantly higher in the TBI group at all observed time points ( $###p < 0.001$ ). Within the TBI group, the 2-day post-injury group showed significantly higher VEGF expression compared to both the 1-day and 3-day groups ( $***p < 0.001$ ). However, there was no significant difference in VEGF expression between the 1-day and 3-day post-injury groups ( $p > 0.05$ ) (Fig. 3).

### Expression and distribution of AQP4 in TP

A small amount of AQP4 expression was observed in glial cells and vascular endothelial cells in both the control and Sham groups, with no significant differences in AQP4 protein content between these groups at any observed time points. On day 1 post-TBI, AQP4 expression increased in both glial cell membranes and vascular endothelial cells, with an accompanying rise in protein content ( $2.65 \pm 0.32$ ). On day 2 post-TBI, AQP4 expression was primarily localized to vascular endothelial cells, and the protein content slightly decreased ( $2.37 \pm 0.28$ ). By day 3 post-TBI, AQP4 was abundantly expressed in glial cells, and protein content significantly increased again ( $4.80 \pm 0.48$ ). Compared with the control and Sham groups, the TBI group showed significantly higher AQP4 protein levels at all time points ( $###p < 0.001$ ). Within the TBI group, AQP4 protein levels on day 3 were significantly higher than those on days 1 and 2 ( $***p < 0.001$ ), while no significant difference was found between days 1 and 2 ( $p > 0.05$ ) (Figs. 4 and 5).

## Discussion

The thalamic peduncle (TP) is a crucial area targeted in the treatment of traumatic brain injury (TBI) patients, closely linked to patient prognosis. Clarifying the molecular pathological changes in TP is fundamental for

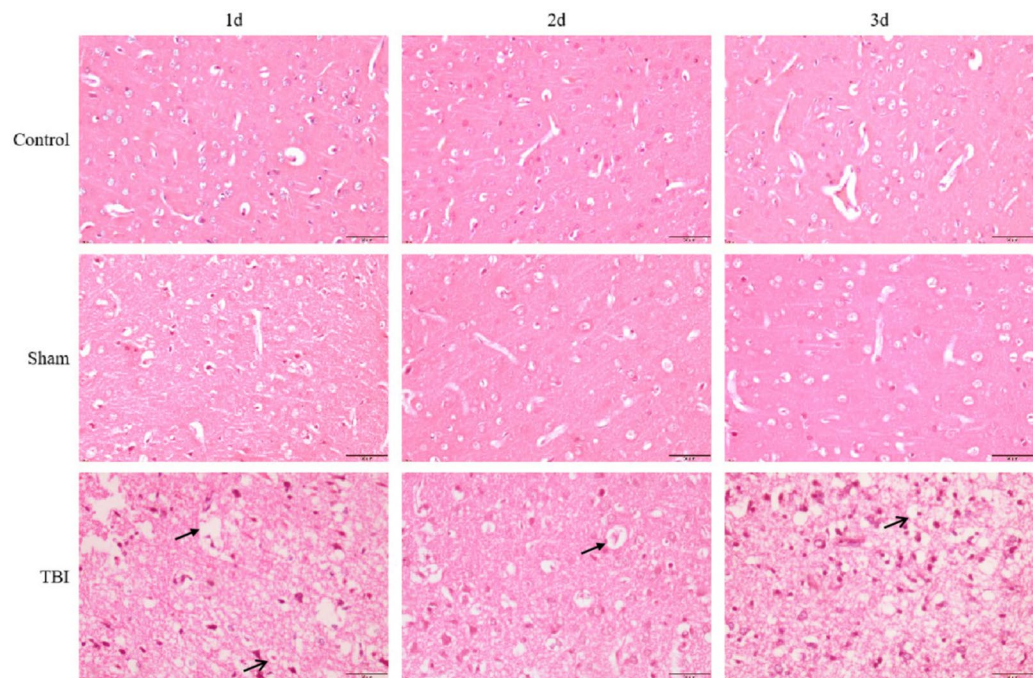


**Fig. 1.** Pathological features of brain tissue in the TP region across different observation time points in each group. Cell morphology and structure appeared normal in both the control and Sham groups. In the TBI group, glial cells exhibited swelling, increased cell volume, transparent and lightly stained cytoplasm, and characteristic vacuolar changes at each time point observed (indicated by black dovetail arrows). Additionally, spaces surrounding vascular endothelial cells were notably widened (indicated by black arrows).

developing targeted therapies for TBI and is the primary aim of this study. We aimed to identify potential therapeutic targets by analyzing the time-dependent pathological characteristics of TP after TBI.

In this study, a rat model of moderate brain trauma was established. Hematoxylin and eosin (HE) staining was first utilized to observe pathological changes in TP at various time points (days 1, 2, and 3) under an optical microscope. We observed cerebral edema at all measured time points, characterized mainly by a mixture of intracellular and vascular edema. However, the dominant type of edema varied over time: intracellular edema prevailed on days 1 and 3, while vascular edema was predominant on day 2. Because observations did not begin immediately after TBI, we could not definitively establish the sequence of edema formation. Nevertheless, existing research indicates vascular edema appears first, as observed one hour after TBI, with intracellular edema developing later<sup>7</sup>. This sequence contrasts with pathological changes observed in the core trauma area<sup>8</sup>, and the reasons for this discrepancy remain unclear.

Vascular edema results from blood-brain barrier (BBB) disruption, increased capillary permeability, and subsequent infiltration of macromolecular proteins and water into the extracellular space. To assess BBB permeability in TP, we measured the levels of immunoglobulin G (IgG), a marker indicating BBB integrity<sup>9</sup>. Our findings revealed significantly elevated IgG levels post-TBI, peaking on day 2 and decreasing slightly on day 3. These results suggest substantial BBB impairment after TBI, with maximal permeability occurring two days post-injury. Comparative analysis of pathological changes in TP indicated that vascular edema correlates strongly with BBB injury, suggesting that BBB disruption plays a central role in the development of brain edema. Studies have confirmed that BBB damage begins within hours post-injury and may persist over extended periods<sup>10</sup>. BBB impairment constitutes a major pathological feature of TBI, linking vascular edema and secondary brain injury<sup>11–13</sup>. Additionally, BBB dysfunction significantly influences injury progression, neuronal repair timelines, and overall patient prognosis. Therefore, targeting BBB repair or stabilization represents a practical therapeutic strategy, potentially more feasible than therapies targeting cells protected by the BBB<sup>14–18</sup>.

BBB permeability is influenced by various factors, with vascular endothelial growth factor (VEGF) being particularly critical<sup>19</sup>. VEGF specifically binds to VEGF receptors (VEGFR) on vascular endothelial cells, inducing increased BBB permeability and subsequent biological responses<sup>20</sup>. To investigate VEGF's role in TP edema following TBI, VEGF protein levels were measured. VEGF content rose significantly on day 1 post-injury, peaked rapidly on day 2, then declined to near day-1 levels by day 3. This pattern closely mirrored the changes in IgG levels, suggesting VEGF's involvement in edema formation by enhancing BBB permeability. The peak in BBB permeability on day 2 may also be attributable to VEGF activity. Thus, inhibiting VEGF expression shortly after TBI might be beneficial in reducing BBB permeability and managing brain edema, highlighting VEGF as another promising therapeutic target. However, differences in the magnitude of VEGF and IgG level fluctuations imply that additional factors likely influence BBB permeability after TBI, with VEGF representing only one component of a broader regulatory mechanism.



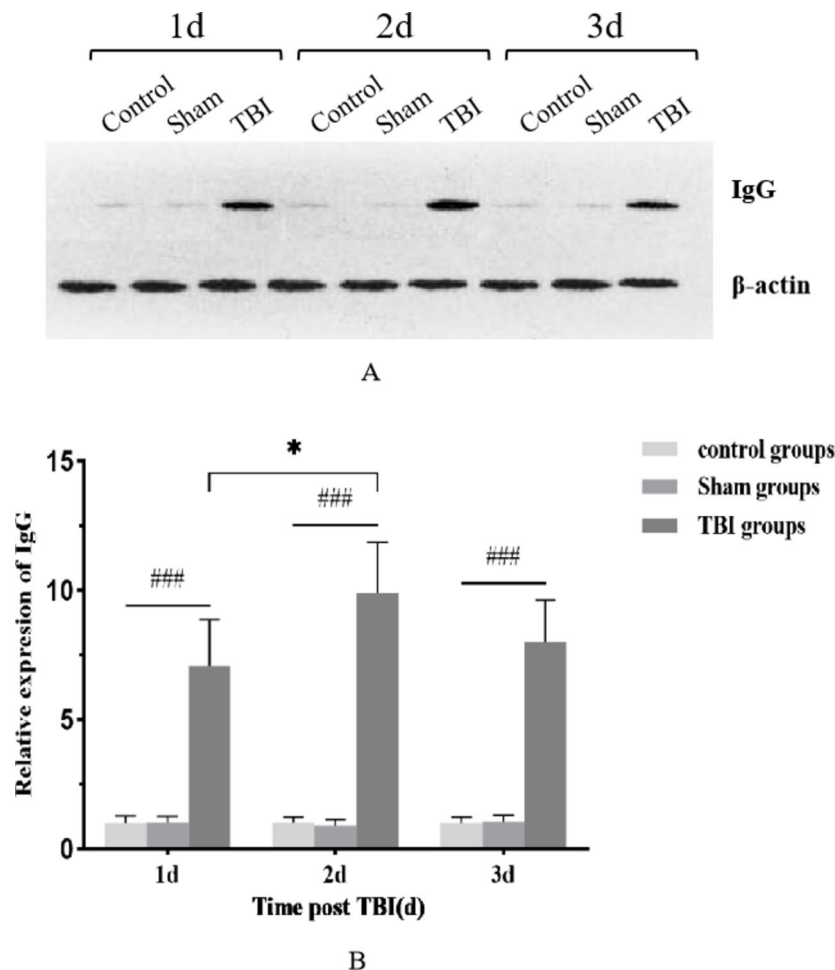


**Fig. 2.** Histogram illustrating the IgG protein content in the TP region at various observation times across groups, accompanied by representative cropped blots from different gels (A,B) ( $N=5$ ). The IgG protein content in the TBI group significantly increased at each observed time point, reaching its peak at 2 days post-injury. ### indicates a significant difference between the TBI group and both the control and Sham groups ( $p < 0.001$ ). \* indicates a significant difference between the 2-day and 1-day post-injury groups within the TBI group ( $p < 0.05$ ).

Aquaporin-4 (AQP4), a transmembrane protein facilitating water transport across cell membranes<sup>21,22</sup>, primarily localizes in vascular endothelial cells, astrocytic endfeet, and supportive cells, significantly influencing traumatic brain edema formation<sup>23,24</sup>. In this study, immunofluorescence and Western blot techniques assessed AQP4 distribution and expression levels in TP. Results showed AQP4 distribution predominantly on glial cell membranes and near vascular endothelial cells on day 1, accompanied by a marked increase in protein levels. By day 2, AQP4 was more concentrated in vascular endothelial cells, with slightly decreased expression. On day 3, AQP4 redistributed primarily to glial cell membranes, and its protein content rapidly peaked again. These findings indicate quantitative increases and regional redistribution of AQP4 post-TBI.

We found a direct relationship between AQP4 expression patterns, edema type, and severity in TP: elevated AQP4 expression and altered polarity correlated with intracellular edema predominance, whereas reduced expression and redistribution were associated with vascular edema prevalence. Therefore, AQP4 is closely linked to the nature and degree of brain edema post-TBI and represents another potential therapeutic target<sup>25–30</sup>. However, studies have shown that silencing AQP4 expression or reversing its distribution effectively mitigates intracellular edema secondary to trauma but has limited effects on vascular edema<sup>31–35</sup>. Consequently, AQP4 targeting may not be universally beneficial across all TBI stages.

Through analyzing the experimental results, we have speculated on the molecular mechanisms underlying cerebral edema formation and development in the thalamic peduncle (TP) during the early stages of traumatic brain injury (TBI). Following brain trauma, external mechanical forces immediately or shortly afterward compromise the structure and function of the blood-brain barrier (BBB), leading to increased permeability. Consequently, water and plasma proteins rapidly accumulate in the extracellular space, initiating vasogenic cerebral edema. Concurrently, cytokines and harmful substances released by immune cells enter the damaged tissue environment through the compromised BBB, exacerbating inflammation, stimulating aquaporin-4

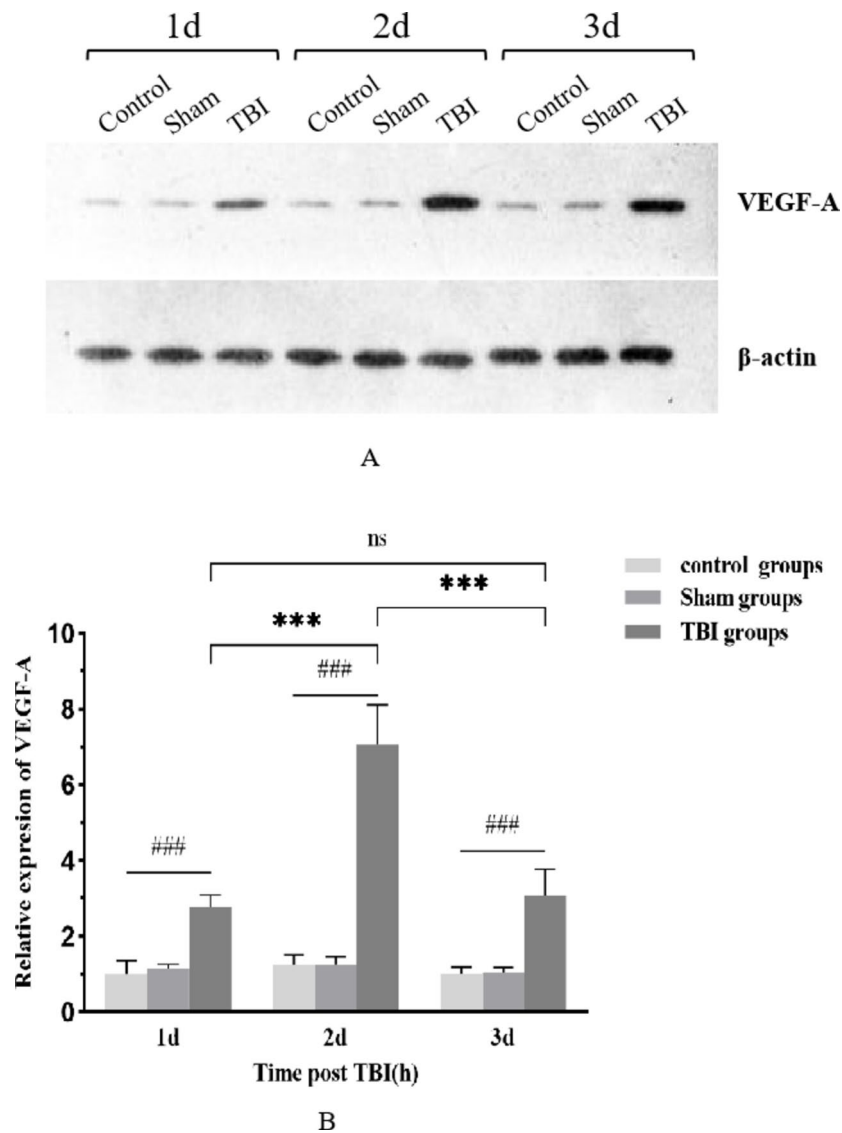


**Fig. 3.** Histogram showing VEGF protein content in the TP region at different observation time points across groups, accompanied by representative cropped blots from different gels (A,B) ( $N=5$ ). VEGF protein content in the TBI group significantly increased at each observed time point, peaking at 2 days post-injury. ### indicates a significant difference between the TBI group and both the control and Sham groups ( $p < 0.001$ ). \*\*\* indicates a significant difference between the 2-day and 1-day post-injury groups within the TBI group ( $p < 0.001$ ). 'ns' indicates no significant difference between the 1-day and 3-day post-injury groups within the TBI group ( $p > 0.05$ ).

(AQP4) transcription and expression, and thereby inducing intracellular edema. This inflammation further exacerbates BBB leakage, aggravating vascular edema<sup>36–38</sup>.

Progressive vascular edema, accompanied by physiological decompensation, elevated intracranial pressure, cerebral ischemia, and hypoxia, impairs sodium-potassium ATPase function. This impairment disrupts osmotic balance, upregulates AQP4 expression, and promotes extensive opening of water channels on glial cell membranes, facilitating the influx of extracellular water and worsening intracellular edema. As a result, both intracellular and vascular edema coexist in the TP region within the first day post-trauma.

Sustained cerebral ischemia and hypoxia further stimulate the expression of hypoxia-inducible factor-1 $\alpha$  (HIF-1 $\alpha$ ), subsequently upregulating vascular endothelial growth factor (VEGF)<sup>39–41</sup>. Highly expressed VEGF directly disrupts BBB tight junctions, activates matrix metalloproteinases to degrade the basement membrane, or binds to VEGFR2 receptors, initiating signaling pathways such as phospholipase C-mediated Ca<sup>2+</sup> influx or PLC $\gamma$ /PKC/eNOS signaling. These pathways elevate nitric oxide (NO) production, further enhancing BBB permeability and exacerbating vascular edema<sup>42–48</sup>. Additionally, increased VEGF promotes angiogenesis, improving cerebral perfusion. However, early-stage neovascularization, characterized by inadequate pericytes and increased vascular permeability, paradoxically enhances vascular edema<sup>49,50</sup>.

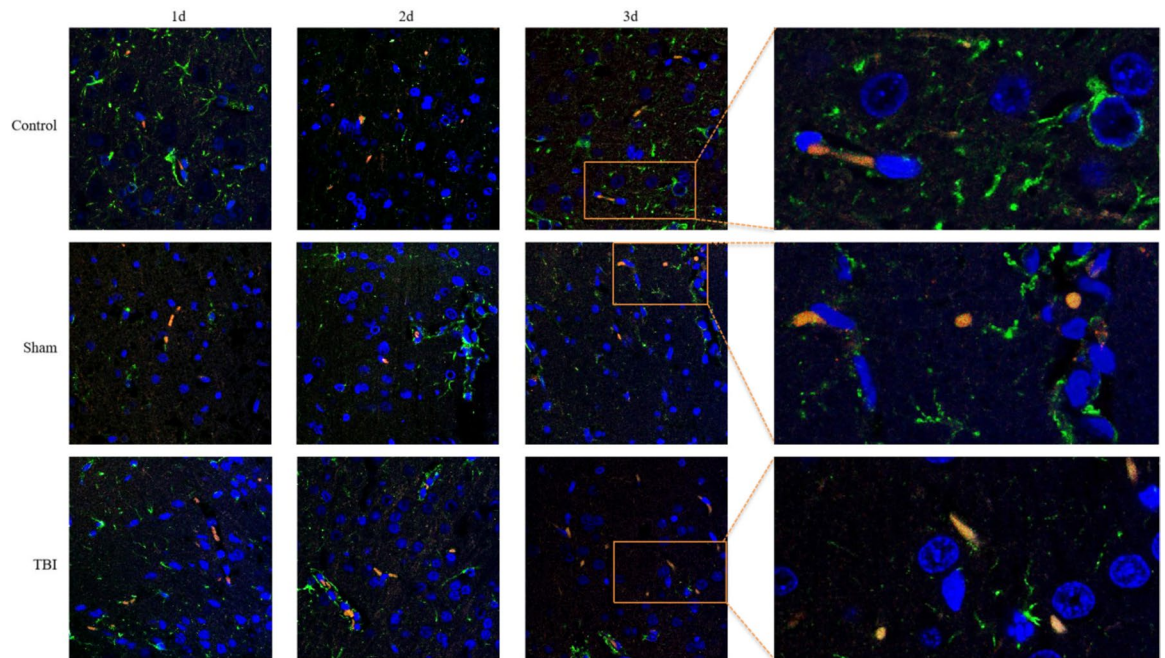


**Fig. 4.** The distribution of AQP4 in each group at different time points was observed by immunofluorescence double labeling. Cell nuclei are marked in blue, GFAP in green, and AQP4 in red.

Subsequently, physiological self-regulation mitigates vascular edema through reduced AQP4 expression and altered protein distribution. Thus, on day two post-trauma, VEGF expression peaks in the TP region, BBB permeability significantly increases, AQP4 expression relatively decreases, and vascular edema predominates. By the third day, although VEGF expression slightly declines and BBB permeability somewhat improves, vascular edema worsens, further exacerbating intracellular edema.

In summary, after brain trauma, compromised BBB integrity in the TP region allows blood-derived substances to infiltrate, increases VEGF expression, and activates various signaling pathways. These combined effects result in vasogenic and intracellular edema, regulated dynamically and interactively by AQP4, culminating in a complex progression of cerebral edema in the TP region (Fig. 6). Therefore, the BBB, VEGF, and AQP4 represent promising therapeutic targets for TBI treatment. Notably, BBB and VEGF are upstream regulatory factors, whereas AQP4 functions downstream. However, these conclusions remain speculative, and further research is necessary to fully elucidate the precise relationships and molecular mechanisms connecting cerebral edema, BBB, VEGF, and AQP4 in the early stages of TBI.

The interaction and mutual influence between vascular edema and intracellular edema create a complex, dynamic process underlying the formation and progression of cerebral edema in the TP region. However, these observations are speculative, and the precise relationships and molecular mechanisms involving cerebral edema, the blood-brain barrier (BBB), vascular endothelial growth factor (VEGF), and aquaporin-4 (AQP4) during the early stages of traumatic brain injury (TBI) require further investigation and confirmation.

## Conclusion

TP is an important target for precise treatment of traumatic brain injury (TBI). During the early stages of TBI, the primary pathological change in TP brain tissue is cerebral edema. Therefore, targeted TBI therapy focuses primarily on addressing brain edema within the TP region. Crucially, the effectiveness of treating brain edema in TP depends on identifying targets that regulate its formation and progression.

In this study, we found that increased blood-brain barrier (BBB) permeability and elevated expression of vascular endothelial growth factor (VEGF) and aquaporin-4 (AQP4) in TP were closely associated with brain edema. This finding suggests that the BBB, VEGF, and AQP4 could serve as potential therapeutic targets for managing brain edema in the TP region. However, it remains unclear whether these three targets are equally effective following TBI or if some may be more suitable at specific times.

Given the complexity of the pathophysiological mechanisms involved in TP, it is possible that additional upstream targets remain unidentified. Exploring these potential targets will guide our future research.

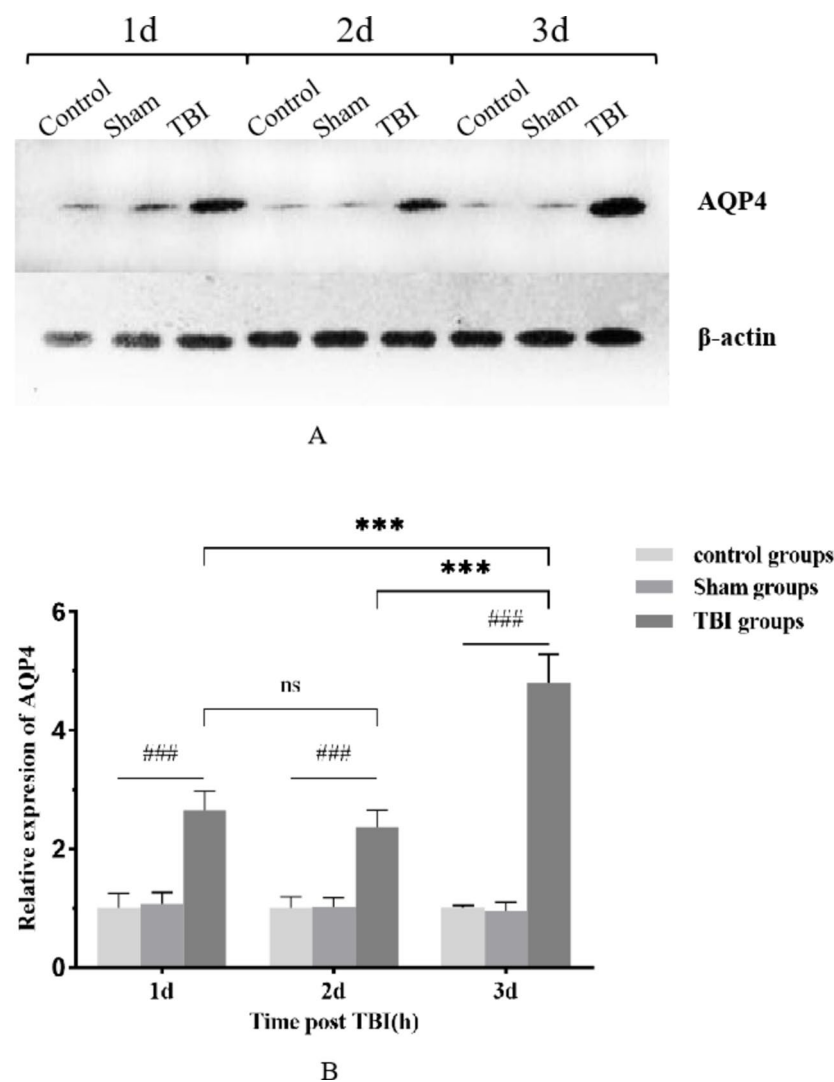


**Fig. 5.** Histogram illustrating the AQP4 protein content in the TP region at different observation time points for each group, accompanied by representative cropped blots from different gels (A,B) ( $N=5$ ). The AQP4 protein content in the TP region of the TBI group significantly increased at each observed time point. ### indicates a significant difference between the TBI group and both the control and Sham groups ( $p < 0.001$ ). \*\*\* indicates a significant difference between the TBI 3-day group and both the 1-day and 2-day post-injury groups within the TBI group ( $p < 0.001$ ). 'ns' indicates no significant difference between the 1-day and 2-day post-injury groups within the TBI group ( $p > 0.05$ ).



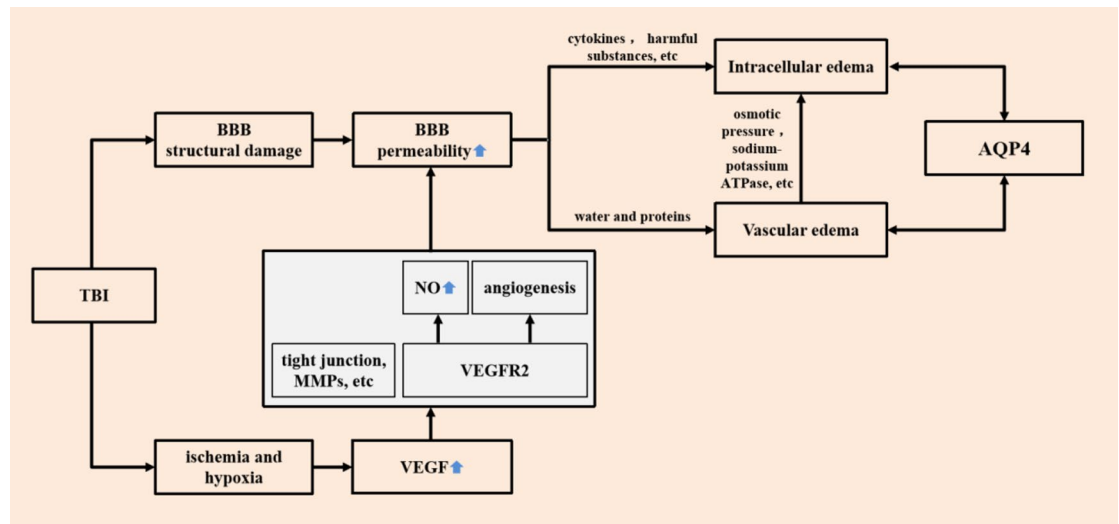


**Fig. 6.** Molecular mechanism derivation diagram for the formation and development of brain edema in the TP region in the early stage of TBI.

### Data availability

The datasets used in the current study are available from the corresponding author on reasonable request.

Received: 2 December 2024; Accepted: 12 May 2025

Published online: 16 May 2025

### References

- Wang, H. et al. TMT-based proteomics analysis to screen potential biomarkers of acute-phase TBI in rats. *Life Sci.* **264**, 118631 (2021).
- van Gils, A. et al. Management of mild traumatic brain injury. *Pract. Neurol.* **20** (3), 213–221 (2020).
- Pitkänen, A. et al. Posttraumatic epilepsy - disease or comorbidity? *Epilepsy Behav.* **38**, 19–24 (2014).
- Dewan, M. C. et al. Estimating the global incidence of traumatic brain injury. *J. Neurosurg.* **130** (4), 1080–1097 (2018).
- Lu, C. et al. Advances in diagnosis, treatments, and mechanistic studies of traumatic brain injury. *Biosci. Trends.* **9** (3), 138–148 (2015).
- Nguyen, R. et al. The international incidence of traumatic brain injury: A systematic review and Meta-Analysis. *Can. J. Neurol. Sci.* **43** (6), 774–785 (2016).
- Ren, H. & Lu, H. Dynamic features of brain edema in rat models of traumatic brain injury. *Neuroreport* **30** (9), 605–611 (2019).
- Feeney, D. M., Boyeson, M. G., Linn, R. T., Murray, H. M. & Dail, W. G. Responses to cortical injury: I. Methodology and local effects of contusions in the rat. *Brain Res.* **211** (1), 67–77 (1981).
- Cash, A. & Theus, M. H. Mechanisms of Blood-Brain barrier dysfunction in traumatic brain Injury. *Int. J. Mol. Sci.* **21** (9), 3344 (2020).
- Hay, J. R., Johnson, V. E., Young, A. M., Smith, D. H. & Stewart, W. Blood-Brain barrier disruption is an early event that May persist for many years after traumatic brain injury in humans. *J. Neuropathol. Exp. Neurol.* **74** (12), 1147–1157 (2015).
- Wei, X. E., Zhang, Y. Z., Li, Y. H., Li, M. H. & Li, W. B. Dynamics of rabbit brain edema in focal lesion and perilesion area after traumatic brain injury: a MRI study. *J. Neurotrauma.* **29** (14), 2413–2420 (2012).
- Jha, R. M., Kochanek, P. M. & Simard, J. M. Pathophysiology and treatment of cerebral edema in traumatic brain injury. *Neuropharmacology* **145** (Pt B), 230–246 (2019).
- Price, L., Wilson, C. & Grant, G. Blood-Brain barrier pathophysiology following traumatic brain injury. In: (eds Laskowitz, D. & Grant, G.) *Translational Research in Traumatic Brain Injury*. Boca Raton (FL): CRC Press/Taylor and Francis Group (2016).
- Sivandzade, F., Alqahtani, F. & Cucullo, L. Traumatic brain injury and Blood-Brain barrier (BBB): underlying pathophysiological mechanisms and the influence of cigarette smoking as a premorbid Condition. *Int. J. Mol. Sci.* **21** (8), 2721 (2020).
- Ho, K. M., Honeybul, S., Yip, C. B. & Silbert, B. I. Prognostic significance of blood-brain barrier disruption in patients with severe nonpenetrating traumatic brain injury requiring decompressive craniectomy. *J. Neurosurg.* **121** (3), 674–679 (2014).
- Alves, J. L. Blood-brain barrier and traumatic brain injury. *J. Neurosci. Res.* **92** (2), 141–147 (2014).
- Hu, Y. & Tao, W. Microenvironmental variations after Blood-Brain barrier breakdown in traumatic brain injury. *Front. Mol. Neurosci.* **14**, 750810 (2021).
- Cho, C. F. et al. Blood-brain-barrier spheroids as an in vitro screening platform for brain-penetrating agents. *Nat. Commun.* **8**, 15623 (2017).
- Wautier, J. L. & Wautier, M. P. Vascular permeability in diseases. *Int. J. Mol. Sci.* **23** (7), 3645 (2022).
- Apte, R. S., Chen, D. S. & Ferrara, N. VEGF in signaling and disease: beyond discovery and development. *Cell* **176** (6), 1248–1264 (2019).
- Assentoft, M., Larsen, B. R. & MacAulay, N. Regulation and function of AQP4 in the central nervous system. *Neurochem. Res.* **40** (12), 2615–2627 (2015).
- Rosito, S. et al. Supramolecular aggregation of aquaporin-4 is different in muscle and brain: correlation with tissue susceptibility in neuromyelitis Optica. *J. Cell. Mol. Med.* **22** (2), 1236–1246 (2018).
- Hinson, S. R., Lennon, V. A. & Pittock, S. J. Autoimmune AQP4 channelopathies and neuromyelitis Optica spectrum disorders. *Handb. Clin. Neurol.* **133**, 377–403 (2016).
- Vogel, A. L. et al. Deletional tolerance prevents AQP4-directed autoimmunity in mice. *Eur. J. Immunol.* **47** (3), 458–469 (2017).

25. Chen, L. H. et al. Interaction of Aquaporin 4 and N-methyl-D-aspartate NMDA receptor 1 in traumatic brain injury of rats. *Iran. J. Basic Med. Sci.* **21** (11), 1148–1154 (2018).
26. Szczygalski, J. et al. Changes in posttraumatic brain edema in Craniectomy-Selective brain hypothermia model are associated with modulation of Aquaporin-4 level. *Front. Neurol.* **9**, 799 (2018).
27. Nekludov, M., Bellander, B. M., Gryth, D., Wallen, H. & Mobarrez, F. Brain-Derived microparticles in patients with severe isolated TBI. *Brain Inj.* **31** (13–14), 1856–1862 (2017).
28. Rodriguez-Grande, B. et al. Gliovascular changes precede white matter damage and long-term disorders in juvenile mild closed head injury. *Glia* **66** (8), 1663–1677 (2018).
29. Jia, J., Chen, F., Wu, Y. & Recombinant PEP-1-SOD1 improves functional recovery after neural stem cell transplantation in rats with traumatic brain injury. *Exp. Ther. Med.* **15** (3), 2929–2935 (2018).
30. Lopez-Rodriguez, A. B., Acaz-Fonseca, E., Viveros, M. P. & Garcia-Segura, L. M. Changes in cannabinoid receptors. *Ne* **10** (6), e0128782 (2015).
31. Li, L. F. et al. The traumatic penumbra of brain injury treated with RNAi: a multimodal magnetic resonance imaging study. *J. Pract. Radiol.* **34** (1), 128–132 (2018).
32. Lu, H., Zhan, Y., Ai, L., Chen, H. & Chen, J. AQP4-siRNA alleviates traumatic brain edema by altering post-traumatic AQP4 Polarity reversal in TBI rats. *J. Clin. Neurosci.* **81**, 113–119 (2020).
33. Glober, N. K. et al. Acetazolamide treatment prevents redistribution of astrocyte Aquaporin 4 after murine traumatic brain injury. *Neurosci. J.* **2019**, 2831501 (2019).
34. Zhang, H. et al. Hypertonic saline improves brain edema resulting from traumatic brain injury by suppressing the NF- $\kappa$ B/IL-1 $\beta$  signaling pathway and AQP4. *Exp. Ther. Med.* **20** (5), 71 (2020).
35. Zhang, Y. et al. Overexpression of long noncoding RNA Malat1 ameliorates traumatic brain injury induced brain edema by inhibiting AQP4 and the NF- $\kappa$ B/IL-6 pathway. *J. Cell. Biochem.* **120** (10), 17584–17592 (2019).
36. Bhowmick, S., D'Mello, V., Caruso, D., Wallerstein, A. & Abdul-Muneer, P. M. Impairment of pericyte-endothelium crosstalk leads to blood-brain barrier dysfunction following traumatic brain injury. *Exp. Neurol.* **317**, 260–270 (2019).
37. Habgood, M. D. et al. Changes in blood-brain barrier permeability to large and small molecules following traumatic brain injury in mice. *Eur. J. Neurosci.* **25** (1), 231–238 (2007).
38. Salehi, A., Zhang, J. H. & Obenaus, A. Response of the cerebral vasculature following traumatic brain injury. *J. Cereb. Blood Flow. Metab.* **37** (7), 2320–2339 (2017).
39. Sharp, F. R. & Bernaudin, M. HIF1 and oxygen sensing in the brain. *Nat. Rev. Neurosci.* **5** (6), 437–448 (2004).
40. Wu, X. et al. Enriched housing promotes post-stroke neurogenesis through Calpain 1-STAT3/HIF-1 $\alpha$ /VEGF signaling. *Brain Res. Bull.* **139**, 133–143 (2018).
41. Wang, K. et al. HIF-1 $\alpha$  and VEGF are involved in Deferoxamine-Ameliorated traumatic brain injury. *J. Surg. Res.* **246**, 419–426 (2020).
42. Cherian, L., Goodman, J. C. & Robertson, C. S. Brain nitric oxide changes after controlled cortical impact injury in rats. *J. Neurophysiol.* **83** (4), 2171–2178 (2000).
43. Davis, B. et al. Role of vasodilator stimulated phosphoprotein in VEGF induced blood-brain barrier permeability in endothelial cell monolayers. *Int. J. Dev. Neurosci.* **28** (6), 423–428 (2010).
44. Fernández-Robredo, P. et al. Effect of lutein and antioxidant supplementation on VEGF expression, MMP-2 activity, and ultrastructural alterations in Apolipoprotein E-deficient mouse. *Oxid. Med. Cell. Longev.* **2013**, 213505 (2013).
45. Huang, L. et al. Hypertonic saline alleviates experimentally induced cerebral oedema through suppression of vascular endothelial growth factor and its receptor VEGFR2 expression in astrocytes. *BMC Neurosci.* **17** (1), 64 (2016).
46. Lin, Y. et al. Blood-brain barrier permeability is positively correlated with cerebral microvascular perfusion in the early fluid percussion-injured brain of the rat. *Lab. Invest.* **92** (11), 1623–1634 (2012).
47. Weis, S. M. & Cheres, D. A. Pathophysiological consequences of VEGF-induced vascular permeability. *Nature* **437** (7058), 497–504 (2005).
48. Ferrara, N., Gerber, H. P. & LeCouter, J. The biology of VEGF and its receptors. *Nat. Med.* **9** (6), 669–676 (2003).
49. Greenberg, J. I. et al. A role for VEGF as a negative regulator of pericyte function and vessel maturation. *Nature* **456** (7223), 809–813 (2008).
50. Andersson, E. et al. Low pericyte coverage of endometrial microvessels in heavy menstrual bleeding correlates with the microvessel expression of VEGF-A. *Int. J. Mol. Med.* **35** (2), 433–438 (2015).

## Author contributions

Experimental design, Ai Li: the conduct of animal experiments, Muhammad Usman: Data collation and analysis. Ai Li writing—original draft preparation. Muhammad Usman; writing—review and editing. Lu Hong, all authors have read and agreed to the published version of the manuscript.

## Funding

Science and Technology Research Project of Chongqing Education Commission (No. KJZD-K202301105).

## Declarations

## Competing interests

The authors declare no competing interests.

## Institutional review board statement

All animal experiments were reviewed and approved by the Institutional Animal Care and Committee of The Seventh People's Hospital of Chongqing (approval number 479/ March 19,2020). All the experiments were carried out in the army special occupational disease prevention and Control Laboratory of Field Surgery Research Department, Army Characteristic Medical Center, Army Medical University. All experimental animals were treated in accordance with GB/T 35892 – 2018 Guidelines for ethical review of the welfare of experimental animals and guidelines for the management and use of experimental animals (8th edition).

## Additional information

**Supplementary Information** The online version contains supplementary material available at <https://doi.org/10.1038/s41598-025-02071-2>.

**Correspondence** and requests for materials should be addressed to H.L.

**Reprints and permissions information** is available at [www.nature.com/reprints](http://www.nature.com/reprints).

**Publisher's note** Springer Nature remains neutral with regard to jurisdictional claims in published maps and institutional affiliations.

**Open Access** This article is licensed under a Creative Commons Attribution-NonCommercial-NoDerivatives 4.0 International License, which permits any non-commercial use, sharing, distribution and reproduction in any medium or format, as long as you give appropriate credit to the original author(s) and the source, provide a link to the Creative Commons licence, and indicate if you modified the licensed material. You do not have permission under this licence to share adapted material derived from this article or parts of it. The images or other third party material in this article are included in the article's Creative Commons licence, unless indicated otherwise in a credit line to the material. If material is not included in the article's Creative Commons licence and your intended use is not permitted by statutory regulation or exceeds the permitted use, you will need to obtain permission directly from the copyright holder. To view a copy of this licence, visit <http://creativecommons.org/licenses/by-nc-nd/4.0/>.

© The Author(s) 2025